Geometrically nonlinear analysis of soil-truss structure interaction

Thiago R. Carvalho[1], Humberto B. Coda[1], Rodolfo A. K. Sanches[1]

[1]*Department of Structural Engineering, EESC, University of São Paulo*
Av. Trabalhador Sãocarlense 400, 13566-590, São Carlos, São Paulo, Brasil
thiagorc7@usp.br, hbcoda@sc.usp.br, rodolfo.sanches@usp.br

Abstract. Soil deformability can cause considerable changes in support reactions and stresses, which are fundamental for the structural design. In turn, the changes in the loads transmitted to the soil causes the deformations presented by the soil to change leading to a coupled problem. This work presents a methodology for numerical analysis of spatial trusses interacting with flexible stratified soils considering geometic nonlinearities. The truss analysis follows a total Lagrangian position-based finite element formulation, while the soil domain analysis is based on fundamental cases of the theory of elasticity considering the characteristics of the soil based on geotechnical field tests. The computational code for dynamic analysis of three-dimensional trusses is verified using analytical and numerical examples from the literature, showing compatible results. In the context of soil mechanics, the model is also verified through examples, considering homogeneous stratified soils with three-dimensional stress propagation. Finally, numerical examples are studied considering the soil-structure interaction, where the influence of the soil-structure interaction on the results is evaluated.

Keywords: Space trusses, soil-structure interaction, three-dimensional stress propagation.

1 Introduction

In the field of Soil-Structure Interaction (SSI), numerical solutions for analyzing these domains have been proposed using the Finite Element Method (FEM), as developed by Farias [5], or by coupling the Boundary Element Method (BEM) with FEM, as demonstrated by Luamba [6], Silva [7], Silva [8], and Ramos [9]. While these techniques are mathematically robust, they come with high computational costs. Therefore, alternative formulations with lower computational costs, such as the one proposed in this work, offer a more viable solution for analyzing the effects of soil-structure interaction in conventional structures and design practice. In this work, we present an analytical-computational solution for the analysis of three-dimensional trusses - soil interaction considering geometric nonlinearities. The proposed formulation aims to be more practical and with lower computational costs than the fully numerical approaches. In this sense, solutions from the Theory of Elasticity are used to evaluate the propagation of stresses in the soil and a total Lagrangian FEM formulation for trusses under small or large displacements is used to describe the structural behavior. Both, structural and soil mechanics models are separatelly verified by numerical examples compared to the literature, and then coupled and tested. The resulting computational code has several practical applications in civil structures, such as the analysis of soil-structure interaction in metal warehouses with trusses, domes with 3D trusses and arches with trusses.

2 Finite element formulation for trusses

The adopted formulation for geometric nonlindear analysis of 3D trusses follows a total Lagrangian description written in terms os current nodal positions, as presented by Coda [1] and Carrazedo [10]. To represent the complete soil-structure problem, we also make use of springs associated to the trusses, so that both, 3D truss and spring elements are represented in Figure 1.

The total mechanical energy functional for the problem, adopting elements with linear approximation, is given by:

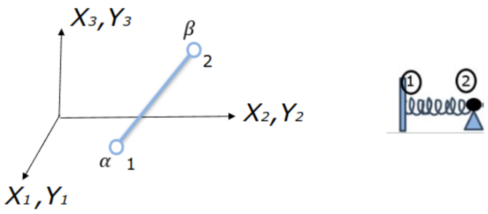

Figure 1. Space truss and spring structural elements.

$$\Pi^h = \Pi^h_{ext} + \Pi^h_{\varepsilon} + \Pi^h_{cin} = -\sum \mathbf{F}_{ext} \cdot \mathbf{y}^h + \sum A_0 l_0 u_{\varepsilon}(\mathbf{y}) + \sum \frac{k_{spring}}{2} (l^{spring} - l_0^{spring})^2 + \sum \frac{1}{2} m \dot{\mathbf{y}}^h \cdot \dot{\mathbf{y}}^h, \quad (1)$$

where $\mathbf{F}_{ext}$ refers to the vector of nodal external forces; $\mathbf{y}^h$ denotes the vector of current positions; A_0 is the truss bar cross-sectional area; l_0 is the length of the truss bar element and u_ε is the specific strain energy of the truss element. Adoppting the Saint-Venant-Kirchhoff constitutive model, we have $u_\varepsilon = \frac{E_{mat}}{2}(\mathbb{E})^2$, with E_{mat} being the modulus of elasticity of the material and $\mathbb{E} = \frac{1}{2}\frac{l^2 - l_0^2}{l_0^2}$ the Green Lagrange strain in the initial axial direction of the element; $\mathbf{y}^h$ denotes the current position; $\dot{\mathbf{y}}^h$ is the current acceleration.

$$\frac{\partial \Pi^h}{\partial Y_{k\beta}} = A_0 S \frac{(-1)^\beta}{l_0}(Y_{k2} - Y_{k1}) + (k_{spring})_{k\beta}(l^{spring} - l_0^{spring}) + \frac{1}{2}\rho A_0 l_0 \ddot{Y}_{k\beta} - F^{ext}_{k\beta} = \mathbf{0}, \quad (2)$$

where $S = E_{mat}\mathbb{E}$ refers to the second Piola-Kirchhoff tensor; k is the direction and β is the node.

3 Soil mechanics

The formulation for the soil analysis is based on an elastic continuum approach to evaluate stress propagation, as described by Pinto [2], Sales [11], and Rauecker [4]. This technique employs Newmark's solution from the Theory of Elasticity to determine the stress value in the soil at a depth z resulting from a surface load applied over an area $a \times b$.

Although soil in general does not exhibit full reversibility after being subjected to deformations as occurs in elastic materials, there is a proportionality between stresses and deformations up to a certain stress level, as postulated by Pinto [2]. Consequently, a constant modulus of elasticity can be considered representative for moderate stress variation levels.

The stress increment at any point is given by $\Delta\sigma = \Delta\sigma_0 I_E$, where I_E is the Newmark factor, and $\Delta\sigma_0$ is the stress increment at the base of the foundation. The factor I_E is calculated as the composition of the Newmark solution: $I_E = I_{EFGH} + I_{EFIK} + I_{EHLJ} + I_{EKDJ}$ for the case of the point internal to the loading area and $I_E = I_{EFGH} - I_{EKLH} - I_{EFIJ} + I_{EKDJ}$ for the external case as shown in Figure 2.

The equation (3) allows you to calculate each of the geometric factors $I_{EFGH}, I_{EFIK}, I_{EHLJ}, I_{EKDJ}, ...$ The incidences EFGH, EFIK, EHLJ, ... indicate the area considered in the surface loading, as illustrated in Figure 2. The factors m and n are directly determined from the definition of this loaded region.

$$I_s = \frac{1}{2\pi}\left[\arctan\left(\frac{m\,n}{\sqrt{m^2+n^2+1}}\right) + \frac{m\,n}{\sqrt{m^2+n^2+1}}\left(\frac{1}{1+m^2} + \frac{1}{1+n^2}\right)\right]. \quad (3)$$

with the m and n factors being symmetrical; the m coefficient is defined as the ratio between the smallest side, b, of the area loaded on the surface and the depth, z; the n factor is defined as the ratio between the largest side, a, and the depth, z.

The (3) equation is the formula for calculating the geometric parameters at the vertices I_{EFGH}, I_{EFIK}, I_{EHLJ}, ... By applying a superposition of effects, a geometric factor I_E can be calculated at any point of interest. In turn, this factor is directly related to the increase in stress at a given depth z by $\Delta\sigma = \Delta\sigma_0 I_E$. Therefore, it

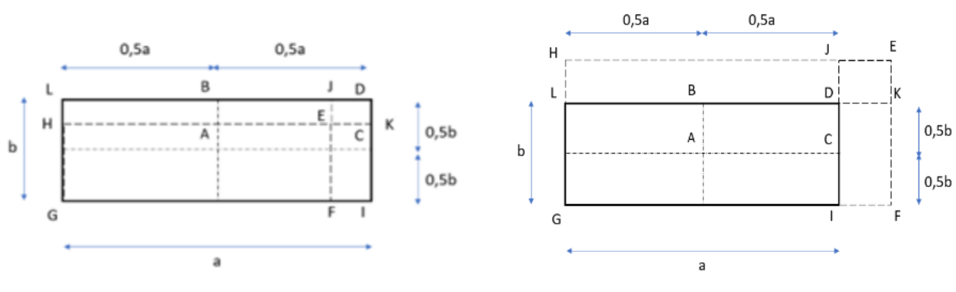

(a) (b)

Figure 2. Composition of the Newmark solution for any position, being (a) for a point inside the loading area; (b) point outside the loading area.

is necessary to make a composition of loading areas, as shown in Figure 2 (a) for internal points and Figure 2 (b) for points external to the support. Configuration (a) is used to evaluate the loads on the support itself, while case (b) is used to determine the stress increase on the other supports. Note that the areas of influence determine the geometric parameters and their composition determines the increase in stress $\Delta\sigma$ at a given depth due to surface loading $\Delta\sigma_0$.

With the value of the total increment in stress at a given depth below the support, the settlement of each support can be determined by

$$r = \sum_{i=1}^{m} \sum_{j=1}^{n} \frac{\Delta\sigma_{ij} \Delta H_{ij}}{E_i}. \tag{4}$$

where r term is the total displacement for any given support. The limits m and n refer respectively to the number of layers in the soil profile of the support, and i to the number of sub-layers in the discretization of layer. The term $\Delta\sigma_{ij}$ refers to the total stress increase (due to the stresses of the support itself and of the others) in layer i of sublayer j. The term ΔH_{ij} refers to the thickness, in layer i, of sub-layer j. Figure 3 illustrates this discretization of soil layers into sub-layers. The term E_i refers to the modulus of elasticity of the soil layer. For more details it is recommended to consult Sales [12], Poulos and Davis [13] and Alves [14].

The total settlement of a support is given by the sum of the total displacements of each layer of the stratified soil profile, while the total settlement of a layer is the result of the sum of the displacements of each sub-layer from the adopted discretization. While the number of layers depends on the soil profile below the support, the number of sub-layers is chosen by the designer in the data input. The greater the number of sublayers, the more refined the procedure.

3.1 Technique for soil-structure coupling

The coupling technique consists of making the stresses of the structure compatible with the geotechnical displacements of the soil. This is done by means of an iterative soil-structure loop that makes the soil displacements predicted by soil mechanics compatible with those applied to the structure. The loop is run until the convergence criterion is reached, i.e. until the residual is minimal. This technique makes it possible to promote the equilibrium of the structure in the deformed condition of the soil, resulting in an analysis of the stresses that is more compatible with reality.

After calculating the settlements using soil mechanics and having the values of the support reactions, it is possible to determine the new displacement field of the structure and the new stiffness matrix of the soil mass. Modifying the stiffness matrix consists of modifying the support conditions a priori, where there is calculated geotechnical settlement and non-displaceable support, the automatic change to an elastic support is performed. With this change, it will be necessary to renumber the degrees of freedom of the structure and recalculate the stiffness matrix of the structure, considering a spring support in place of the initial non-displaceable support.

These new matrices are calculated internally in the program from the modification of the support conditions, followed by the application of the functions for assembling the degrees of freedom of the structure and the stiffness matrix of the structure, considering the new state of the structure with spring support. The coefficients of these

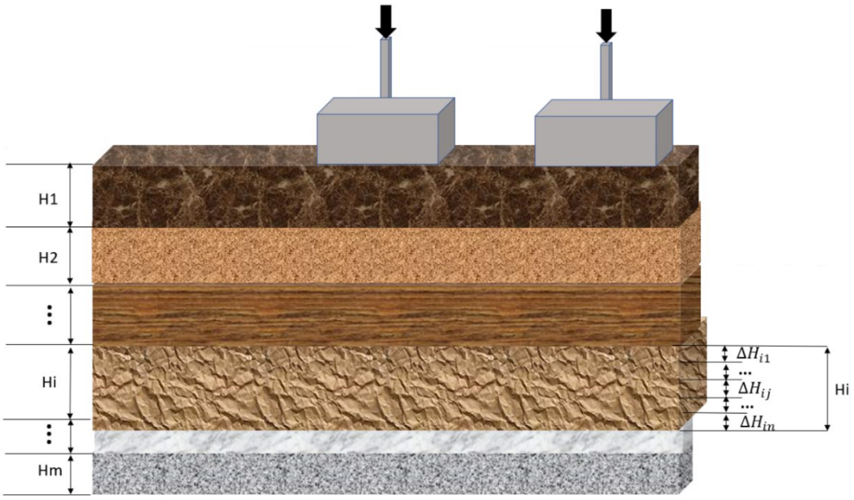

Figure 3. Discretization of the stratified soil mass.

springs are also calculated automatically, from the relationship between the support reactions and the geotechnical settlements. With the values of the settlements imposed on the supports updated, the modification of the other dependent matrices can be carried out by calling the assembly functions of such matrices. Therefore, the program promotes the interaction between the soil and the structure in a partitioned manner, seeking equilibrium in the deformed condition of the soil.

4 Results and analysis

This section presents the results of the computational implementation. The structural formulation for space trusses has been implemented and verified for large displacements and in terms of 3D geometry. The code for the soil was checked in terms of the total settlement in the foundation. At the end, an example of Soil-Structure Interaction is presented in a 3D dome balancing the deformed condition of the structure and the soil.

4.1 Structural analysis

Figure 4 (a) shows a pendulum that will be used to check the non-linear implementation of the structure. Using a truss bar with high stiffness and negligible mass, it is possible to simulate this problem with the implemented truss program. Figure 4 (b) shows that the results obtained are compatible with the analytical non-linear solution.

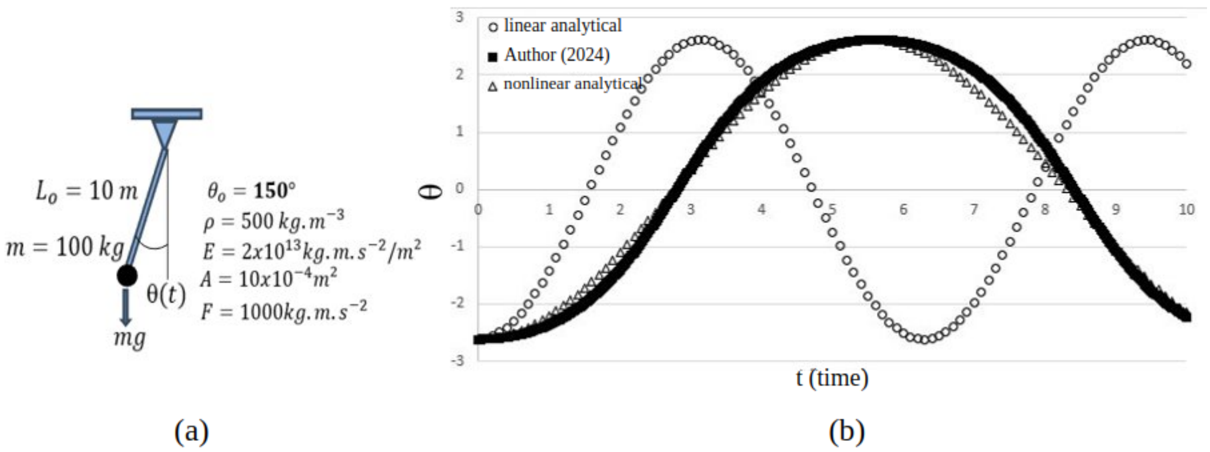

Figure 4. Nonlinear pendulum modeled by the implemented truss program

Figure 5 shows an example for three-dimensional verification of the implementation. The displacement in the center was calculated as 1.14869 x $10^{-4}m$. The same result was obtained in the LESM program, resulting in good indications for the implementation made.

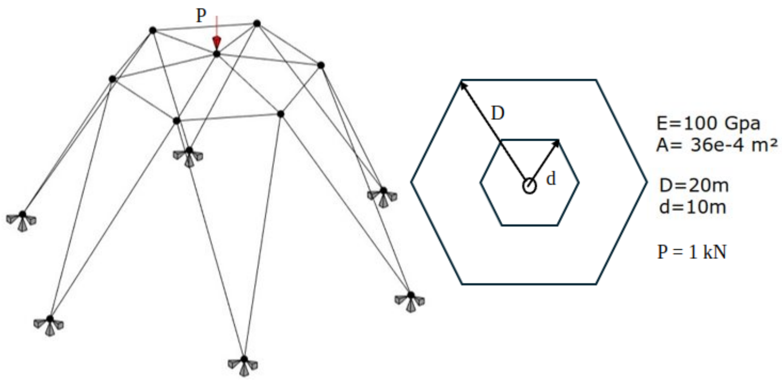

Figure 5. Dome with 3D truss

4.2 Soil analysis

Figure 6 shows an example of a stratified soil profile for checking soil implementation. The displacement of the 15 m massif was calculated as 19.19 mm, 99% compatible with the reference value of 19.18 mm given by Sales [11].

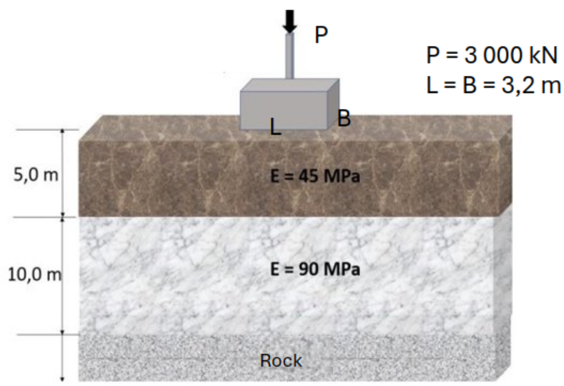

Figure 6. Implementation Verification for Stratified Soils

4.3 Soil-structure interaction analysis

Figure 7 (a) shows an example for the analysis of soil-structure interaction. The structure model is the same as the dome in Figure 5. The soil profile used is relative to a real case used in the calculation of the foundation of a 34-storey building located in the Marista sector of Goiânia (Goiás in Brazil) as described by MUNDIM et al. [3]. Figure 7 (b) shows the structure in the deformed configuration. It is noted that the supports also move, depending on the deformation of the soil. In this sense, the structure is in equilibrium both in its own deformed configuration and in that of the soil, resulting in a model that is more compatible with the boundary conditions of a structure.

In addition to analyzing the displacement field, the spring coefficients compatible with this geometry and the given soil profile were also calibrated. The k_{spring} = 1.638x 10^5 N/m results in a mechanical analog for the deformation of the soil with this structural topology. Note that this value depends not only on the soil profile, but also on the structural configuration, and is only obtained at the end of equilibrium in the deformed condition.

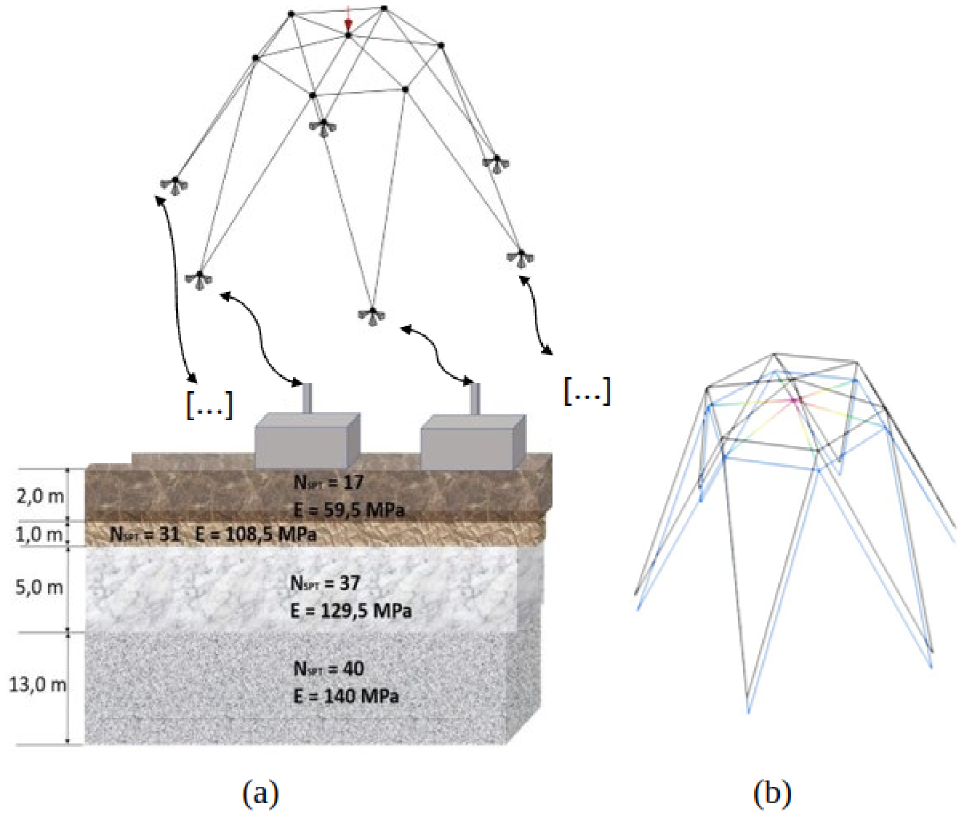

Figure 7. Example for the analysis of soil-structure interaction.

5 Conclusions

The proposed methodology for geometrically nonlinear analysis of soil-truss structure interaction considering a finite element formulation for 3D trusses dynamics coupled to a analytical model for soil mechanics revealed to be a relatively simple, practical and robust tool. From the results presented, one can observe that the finite element formulation adopted for describing the spatial trusses is robust and suitable for the scope of soil-structure interaction. On the other hand, adopting a simplified model based on the theory of elasticity for the soil ensures low computational cost and practicity to the resulting computational code. Furthermore, the spring coefficient calibration allows obtaining precise mechanical models for the analysis of SSI.

Acknowledgements. This study was financed in part by the Coordenação de Aperfeiçoamento de Pessoal de Nível Superior - Brasil (CAPES) - finance code 001 and by Brazilian National Council for Research and Technological Development (CNPq) - grant -314045/2023-6.

Authorship statement. The authors hereby confirm that they are the sole liable persons responsible for the authorship of this work, and that all material that has been herein included as part of the present paper is either the property (and authorship) of the authors, or has the permission of the owners to be included here.

References

[1] H. B. Coda. *O Método dos elementos finitos posicional: sólidos e estruturas - não linearidade geométrica e dinâmica*. EESC/USP, São Carlos, 2018.
[2] C. S. Pinto. *Curso Básico de Mecânica dos Solos*. Oficina de Textos, São Paulo, 2006.
[3] D. P. R. MUNDIM, E. CRUVINEL, and M. CAVALCANTI. *Implementação de uma Ferramenta Numérica para Previsão de Recalques em Sapatas*. UFG, 2014.
[4] J. C. N. Rauecker. *Previsão do recalque de um edifício alto com fundação em sapata na cidade de Goiânia*. UFG, Universidade Federal de Goiás, Escola de Engenharia Civil e Ambiental, Goiânia, 2018.

[5] R. S. Farias. *Análise estrutural de edifícios de paredes de concreto com a incorporação da interação solo-estrutura e das ações evolutivas*. PhD thesis, Escola de Engenharia de São Carlos, Universidade de São Paulo, São Carlos, 2018.

[6] E. S. Luamba. *Formulação MEC/MEF para a Análise da Interação Solo Estratificado/Estrutura e da Estabilidade da Estaca*. PhD thesis, Escola de Engenharia de São Carlos, Universidade de São Paulo, São Carlos, 2022.

[7] R. C. S. Silva. Análise da interação estaca inclinada e o solo via combinação mec/mef. Master's thesis, Escola de Engenharia de São Carlos, Universidade de São Paulo, São Carlos, 2020.

[8] W. Q. Silva. *Sobre análise não linear geométrica de edifícios considerando o empenamento dos núcleos estruturais e a interação solo-estrutura*. PhD thesis, Escola de Engenharia de São Carlos, Universidade de São Paulo, São Carlos, 2014.

[9] A. P. F. Ramos. *Análise da interação estaca-solo-superestrutura com o acoplamento MEC-MEF*. PhD thesis, Escola de Engenharia de São Carlos, Universidade de São Paulo, São Carlos, 2013.

[10] R. Carrazedo. *Estudo e desenvolvimento de código computacional para análise de impacto entre estruturas levando em consideração efeitos térmicos*. PhD thesis, Escola de Engenharia de São Carlos, Universidade de São Paulo, São Carlos, 2009.

[11] M. M. Sales. *Fundações: Recalques em Sapatas Sobre Areias e Argilas*. UFG, Universidade Federal de Goiás, Escola de Engenharia Civil e Ambiental, Goiânia, 2022.

[12] M. M. Sales. *Análise do Comportamento de Sapatas Estaqueadas*. PhD thesis, Departamento de geotecnia, Universidade de Brasília, Brasília, 2000.

[13] H. G. Poulos and E. H. Davis. *Pile Foundation Analysis and Design*. Sydney, 1976.

[14] K. C. S. K. Alves. *Previsão de recalques com interação entre sapatas/radiers*. Escola de Engenharia Civil e Ambiental, Universidade Federal de Goiás, Goiânia, 2013.